with B42-SHP expressed 1 U of β-galactosidase.
14. B. M. Forman, K. Umesono, J. Chen, R. M. Evans, *Cell* **81**, 541 (1995).
15. T. Perlmann and L. Jansson, *Genes Dev.* **9**, 769 (1995).
16. P. L. Hallenbeck, M. S. Marks, R. E. Lippoldt, K. Ozato, V. M. Nikodem, *Proc. Natl. Acad. Sci. U.S.A.* **89**, 5572 (1992).
17. T. H. Bugge, J. Pohl, O. Lonnoy, H. G. Stunnenberg, *EMBO J.* **11**, 1409 (1992).
18. S. A. Kliewer, K. Umesono, D. J. Mangelsdorf, R. M. Evans, *Nature* **355**, 446 (1992).
19. M. Leid *et al.*, *Cell* **68**, 377 (1992).
20. X.-K. Zhang, B. Hoffmann, P. B.-V. Tran, G. Graupner, M. Pfahl, *Nature* **355**, 441 (1992).
21. R. Benezra, R. L. Davis, D. Lockshon, D. L. Turner, H. Weintraub, *Cell* **61**, 49 (1990).
22. B. L. Kreider, R. Benezra, G. Rovera, T. Kadesch, *Science* **255**, 1700 (1992).
23. S. Pesce and R. Benezra, *Mol. Cell. Biol.* **13**, 7874 (1993).
24. T. E. Wilson, T. J. Fahrner, J. Milbrandt, *ibid.*, p. 5794.
25. H. P. Harding and M. A. Lazar, *ibid.*, p. 3113.
26. V. Giguere *et al.*, *Genes Dev.* **8**, 538 (1994).
27. F. M. Ausubel *et al.*, Eds., *Current Protocols in Molecular Biology* (Greene, New York, 1995).
28. Abbreviations for the amino acid residues are as follows: A, Ala; C, Cys; D, Asp; E, Glu; F, Phe; G, Gly; H, His; I, Ile; K, Lys; L, Leu; M, Met; N, Asn; P, Pro; Q, Gln; R, Arg; S, Ser; T, Thr; V, Val; W, Trp; and Y, Tyr.
29. W. A. Seagraves and D. S. Hogness, *Genes Dev.* **4**, 204 (1990).
30. M. Au-Fliegner, E. Helmer, J. Casanova, B. M. Raaka, H. H. Samuels, *Mol. Cell. Biol.* **13**, 5725 (1993).
31. E. D. Rosen, E. G. Beninghof, R. J. Koenig, *J. Biol. Chem.* **268**, 11534 (1993).
32. W. Bourget, M. Ruff, P. Chambon, H. Gronemeyer, D. Moras, *Nature* **375**, 377 (1995).
33. The intact SHP clone was fused to a derivative of the pGEX series of GST expression vectors, and the GST-SHP fusion protein or GST alone was expressed in *Escherichia coli* as described (*27*). Receptors and luciferase were expressed by in vitro translation, and protein interaction tests were done as described (*6*), except that ^{35}S-labeled proteins were precleared by incubation with GST alone bound to glutathione–Sepharose-4B beads. After centrifugation, the supernatant was incubated with GST-SHP or GST protein. Specifically bound proteins were eluted from beads with 40 mM reduced glutathione in 50 mM tris (pH 8.0).
34. H. de The, M. Vivanco-Ruiz, P. Tiollais, H. Stunnenberg, A. Dejean, *Nature* **343**, 177 (1990).
35. H. M. Sucov, K. K. Murakami, R. M. Evans, *Proc. Natl. Acad. Sci. U.S.A.* **87**, 5392 (1990).
36. R. F. Selden, K. B. Howie, M. E. Rowe, H. M. Goodman, D. D. Moore, *Mol. Cell. Biol.* **6**, 3173 (1986).
37. We thank T. Gulick for helpful discussions, receptor expression vectors, and reporter constructs, D. Simha for RAR protein, and B. Forman and R. M. Evans for plasmids for the mammalian two-hybrid system. W.S. was supported by a fellowship from the Helen Hay Whitney Foundation. Supported by grant DK46546 from the NIH to D.D.M.

7 November 1995; accepted 5 March 1996

PKD2, a Gene for Polycystic Kidney Disease That Encodes an Integral Membrane Protein

Toshio Mochizuki, Guanqing Wu,* Tomohito Hayashi,* Stavroulla L. Xenophontos, Barbera Veldhuisen, Jasper J. Saris, David M. Reynolds, Yiqiang Cai, Patricia A. Gabow, Alkis Pierides, William J. Kimberling, Martijn H. Breuning, C. Constantinou Deltas, Dorien J. M. Peters, Stefan Somlo†

A second gene for autosomal dominant polycystic kidney disease was identified by positional cloning. Nonsense mutations in this gene (*PKD2*) segregated with the disease in three PKD2 families. The predicted 968–amino acid sequence of the *PKD2* gene product has six transmembrane spans with intracellular amino- and carboxyl-termini. The PKD2 protein has amino acid similarity with PKD1, the *Caenorhabditis elegans* homolog of PKD1, and the family of voltage-activated calcium (and sodium) channels, and it contains a potential calcium-binding domain.

Autosomal dominant polycystic kidney disease (ADPKD) accounts for 8 to 10% of all end-stage renal disease worldwide (*1*). Its principal clinical manifestation is bilateral renal cysts that result in chronic renal failure in about 45% of affected individuals by age 60 (*1*). Hypertension and liver cysts are common, and the involvement of other organ systems (*2*) lends support to the view that polycystic kidney disease is a systemic disorder (*1*). Genetic heterogeneity in ADPKD has been demonstrated after linkage was initially discovered for the gene on chromosome 16p13.3 (*PKD1*) (*3*, *4*). The second gene, *PKD2*, has been localized on chromosome 4q21-23 and accounts for approximately 15% of affected families (*5*, *6*). At least one more gene for ADPKD is known to exist (*4*). Clinical studies have demonstrated a milder phenotype for the non-PKD1 forms (*7*). This report describes the positional cloning (*8*) of a candidate gene in which truncating mutations have been identified in three PKD2 families (*9*).

The *PKD2* genetic interval is flanked by the polymorphic markers D4S231 and D4S414/423 (*5*). We constructed a yeast artificial chromosome (YAC) contig and high-density sequence tag site (STS) map of this region (*10*) (Fig. 1). Genetic studies in affected families using physically ordered polymorphic markers led to several progressive refinements of the *PKD2* interval (*11*, *12*). The closest unambiguous flanking genetic markers are AFMa059xc9 proximally and AICA1 distally (Fig. 1, A and B) (*10*). We constructed a cosmid- and P1-based (*13*) contig extending over ~680 kb from AICA1 to the region centromeric to the polymorphic marker JSTG3 (Fig. 1C) (*14*). This contig contains a single gap of less than 40 kb. Complementary DNAs corresponding to genes in this region were isolated with inserts from the genomic clones used to screen either a human fetal brain or adult kidney cDNA library (*15*). The mapping of the cDNA clones identified was confirmed, and the clones were sequenced. These sequences were analyzed to identify open reading frames (ORFs), and database searches with the BLAST algorithms (*16*) were performed.

One group of cDNA clones, collectively termed cTM-4, were initially isolated with insert DNA from cosmid c44a9 from the chromosome 4–specific cosmid library (Fig. 1D) (*13*, *15*). None of the cTM-4 clones have homology at the nucleotide level to any known genes, although two randomly sequenced cDNA clones were identified (Fig. 1E). Northern (RNA) blot hybridization with the cTM-4B3-3 insert (Fig. 1E) revealed a ~5.4-kb transcript expressed in most fetal and adult tissues (Fig. 2). cTM-4 is strongly expressed in ovary, fetal and adult kidney, testis, small and large intestine, and fetal lung. Peripheral blood leukocytes were the only tissue tested in which expression was not detected.

Initial database searches with the six translated reading frames obtained from the sequence of clone cTM-4B3-3 revealed homology at the amino acid level with the *PKD1* gene product also called polycystin (*17*, *18*). On the basis of its map location, pattern of expression, and the observed homology, the cTM-4 gene was further investigated as a candidate for *PKD2*. Nine over-

T. Mochizuki, G. Wu, T. Hayashi, D. M. Reynolds, Y. Cai, S. Somlo, Renal Division, Department of Medicine and Molecular Genetics, Albert Einstein College of Medicine, 1300 Morris Park Avenue, Bronx, NY 10461, USA.
S. L. Xenophontos and C. C. Deltas, Cyprus Institute of Neurology and Genetics, 6 International Airport Avenue, 2012 Agios Dhomentios, Nicosia, Cyprus.
B. Veldhuisen, J. J. Saris, M. H. Breuning, D. J. M. Peters, Department of Human Genetics, Sylvius Laboratories, Leiden University, Wassenaarseweg 72, 2333 AL, Leiden, Netherlands.
P. A. Gabow, Department of Internal Medicine, Colorado University Health Sciences Center, Denver, CO 80220, USA.
A. Pierides, Department of Nephrology, Nicosia General Hospital, 1311 Nicosia, Cyprus.
W. J. Kimberling, Departments of Pathology and Otolaryngology, Boys Town National Research Hospital, Omaha, NE 68131, USA.
*These authors contributed equally to this work.
†To whom correspondence should be addressed.

lapping cDNA clones were completely sequenced in both directions (Fig. 1E). The 5′ end of the cTM-4 gene contains a pair of genomic Not I sites, and the 3′ end extends in the telomeric direction beyond the end of the P1 clone p157n2 into cosmid c44a9 (Fig. 1, C and D). The gene extends over 68 kb of the genome.

The consensus 5057–base pair (bp) sequence (*19*) is represented schematically in Fig. 1E. A translation start site with a good Kozak consensus sequence (5′-ACCGCGATGG-3′) (*20*) was identified 67 bp from the 5′ end of the K1-1 clone and 61 bp after an in-frame stop codon. It is followed by a 2904-bp ORF followed, in turn, by several in-frame stop codons. The 3′ untranslated region is 2086 bp long and contains a consensus polyadenylation signal.

We next analyzed the DNA sequence and expression profiles of cTM-4 in unrelated affected individuals from PKD2 families (*3*, *5*, *12*). We used reverse-transcribed RNA and genomic DNA templates to generate polymerase chain reaction (PCR) products for single-strand conformational analysis (SSCA) (*21*). Genomic PCR products of SSCA variants identified in three families were subjected to direct sequencing. Each affected individual was found to be heterozygous for a single base change that resulted in a nonsense mutation (Fig. 3) (*21*). The mutation in family 97 is a G-to-A transition in the codon for Trp^{380} (Figs. 3 and 4). The mutations in the Cypriot families 1605 and 1601 are C-to-T transitions in codons Arg^{742} and Gln^{405}, respectively (Figs. 3 and 4). Using either the resultant loss of a restriction site in families 97 and 1605 or the SSCA pattern in family 1601, we were able to demonstrate segregation of the mutation with the disease phenotype in each family (Fig. 3) (*21*). Analysis of between 90 and 100 normal chromosomes failed to show the predicted affected allele in any case, making it less likely that these sequence differences represent anonymous polymorphisms (*10*). These limited findings do not provide evidence for clustering of mutations in *PKD2*.

The identification of mutations that disrupt the predicted translation product of cTM-4 and the segregation of these mutations with the ADPKD phenotype in three well-characterized PKD2 pedigrees provide strong evidence that cTM-4 is the *PKD2* gene. The putative translation product of the cTM-4 ORF is a 968–amino acid sequence with a calculated molecular mass of 110 kD. Modeling with several hydrophobicity algorithms (*22*) suggests that cTM-4 is an integral membrane protein with six (range, five to eight) membrane-spanning domains and intracellular NH_2- and COOH-termini (*23*). Of the six highest scoring domains, the fourth transmembrane domain (tm4, Fig. 4) produced the lowest scores but was consistently predicted to be a membrane span by several analyses (*22*). The positive inside rule (*23*)—that positively charged amino acids usually face the cytoplasm in transmembrane proteins—strongly supports the predicted topology. The majority of the *N*-glycosylation sites, occurring in the segment between tm1 and tm2 (Fig. 4), are predicted to be extracellular. In addition, potential phosphorylation sites were identified primarily in the COOH-terminal region, as was a putative EF-hand domain (*24*), and this region is predicted to be intracellular (Fig. 4). If a stable protein product is produced, the mutations in families 97 and 1601 are expected to result in a product with an intact intracellular NH_2-terminal domain, first transmembrane domain, and part of the first extracellular loop. The mutation in family 1605 is predicted to result in a product lacking the portion of the intracellular COOH-terminus that contains several phosphorylation sites and

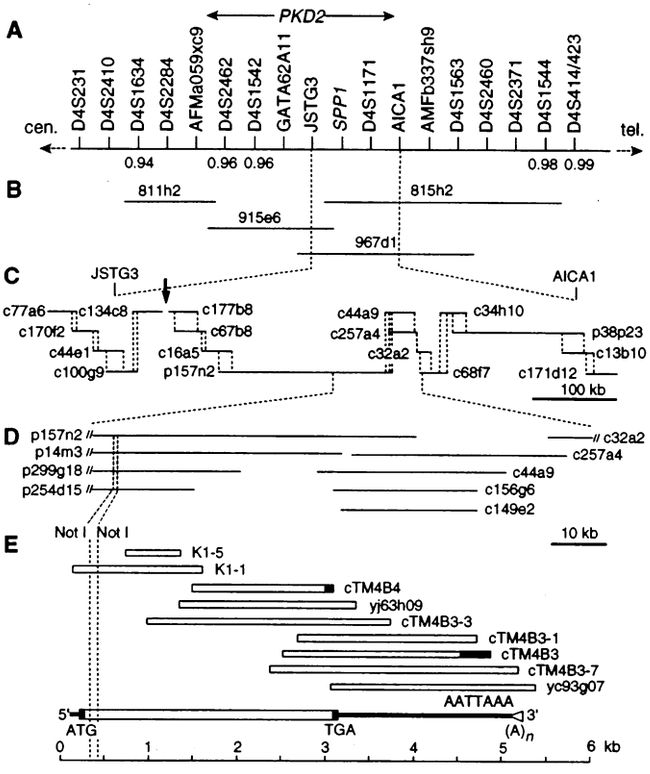

Fig. 1. Positional cloning of *PKD2*. (**A**) Subset of STSs from the high-density map of the *PKD2* region showing polymorphic loci flanking the interval. JSTG3 and AICA1 are two of nine microsatellite markers in this region developed by our groups (*10*). *SPP1* (osteopontin, STS4-1078) and D4S1171 were used to screen the P1 library (*13*, *14*). Other sources of STSs include published linkage maps and genome center databases. cen., centromere; tel., telomere. Distances are in Morgans along chromosome 4. (**B**) Representative mega-YACs (*30*) and their STS content. The mega-YACs form a contig around the *PKD2* region. (**C**) Minimum tiling path of the cosmid and P1 contig in the *PKD2* region (*14*). Clone names beginning with "c" and "p" refer to cosmid and P1 clones, respectively; addresses are from the original arrayed libraries (*13*). The clones containing JSTG3 and AICA1 are shown; a single gap of <40 kb is indicated by the arrow. (**D**) Detail of the portion of the contig containing the *PKD2* candidate gene, cTM-4. (**E**) Overlapping map of nine cDNA clones for cTM-4 and a composite schematic at the bottom. Clones K1-1 and K1-5 are from the adult kidney library; clones yj63h09 and yc93g07 were identified by GenBank searching and are from the normalized infant brain library (*31*); all other clones are from the fetal brain library (*15*). Shaded areas represent chimeric portions of clones.

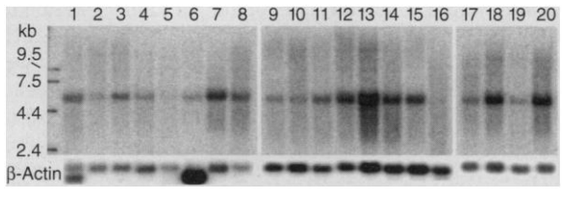

Fig. 2. Expression of the *PKD2* candidate gene. The insert from cTM-4B3-3 (Fig. 1E) was used as a hybridization probe on mRNA blots containing human tissues (Clonetech, Palo Alto, California). Hybridization was as described (*14*) without pre-competition and with a final wash stringency of 0.5× SSC and 0.1% SDS at 65°C. Tissues in numbered lanes are as follows: (1) heart, (2) brain, (3) placenta, (4) lung, (5) liver, (6) skeletal muscle, (7) kidney, (8) pancreas, (9) spleen, (10) thymus, (11) prostate, (12) testis, (13) ovary, (14) small intestine, (15) colon, (16) leukocytes, (17) fetal brain, (18) fetal lung, (19) fetal liver, and (20) fetal kidney. At the bottom, β-actin hybridization to the same blots is used to compare relative mRNA loading within each blot.

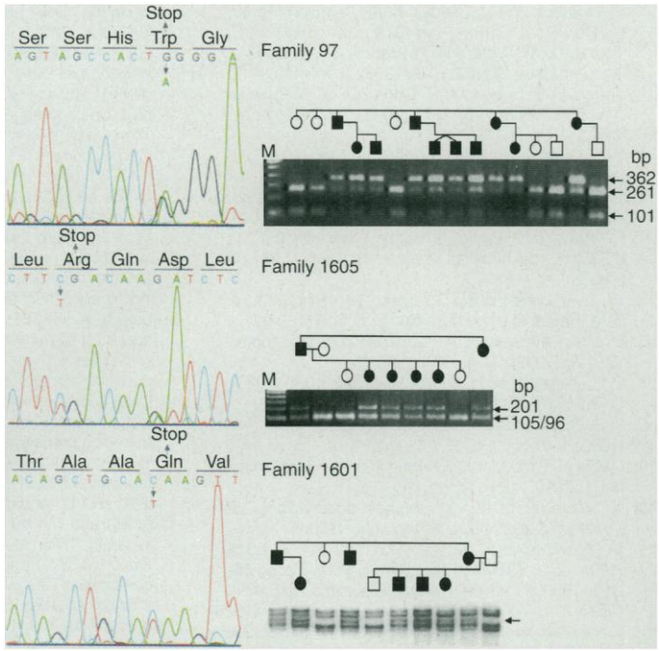

Fig. 3. Mutations in *PKD2*. Analysis of genomic PCR products (*21*) in three *PKD2* families. The left panel shows the results of direct sequencing of genomic PCR products from affected individuals. The arrows denote double peaks, confirmed by sequencing in both directions, indicative of heterozygosity at that nucleotide. Each of the mutant alleles results in a premature stop codon. The right panel demonstrates segregation of the mutated allele with the disease phenotype. In families 97 and 1605, the affected alleles are not digested by Bsr I and Taq I, respectively, because the restriction sites are lost by mutation (*21*). Family 1601 shows segregation of the SSCA variant, indicated by the arrow, with the disease phenotype (*21*). For each family, only portions of more extensive pedigrees are shown. Filled symbols, affected individuals; open symbols, unaffected individuals; M, 100-bp ladder.

the EF-hand domain (Fig. 4).

There is ~25% identity and ~50% similarity between the putative translation product of *PKD2* and ~450 amino acids of PKD1 and its *Caenorhabditis elegans* homolog, ZK945.9 (Fig. 4). There is a comparable degree of similarity with ~270 residues of the voltage-activated Ca^{2+} channel α_{1E} (VACC$\alpha_{1E\text{-}1}$; Fig. 4). The similarity between PKD2 and PKD1 (and ZK945.9) extends over the region tm1 to tm6 in PKD2 but does not include the NH_2- and COOH-terminal domains. The corresponding region of PKD1 has been predicted to contain four transmembrane segments (*18*), three of these corresponding to tm1, tm2, and tm5 in PKD2 and the fourth localizing between tm5 and tm6 of PKD2. The regions corresponding to tm3 and tm4 of PKD2 were not predicted to be membrane spans in that report (*18*).

The similarity to VACC$\alpha_{1E\text{-}1}$ (*25*) is presented as the strongest example of a general homology of PKD2 to the family of voltage-activated Ca^{2+} and Na^+ α_1 channel proteins. These channel proteins contain four homologous domains (I through

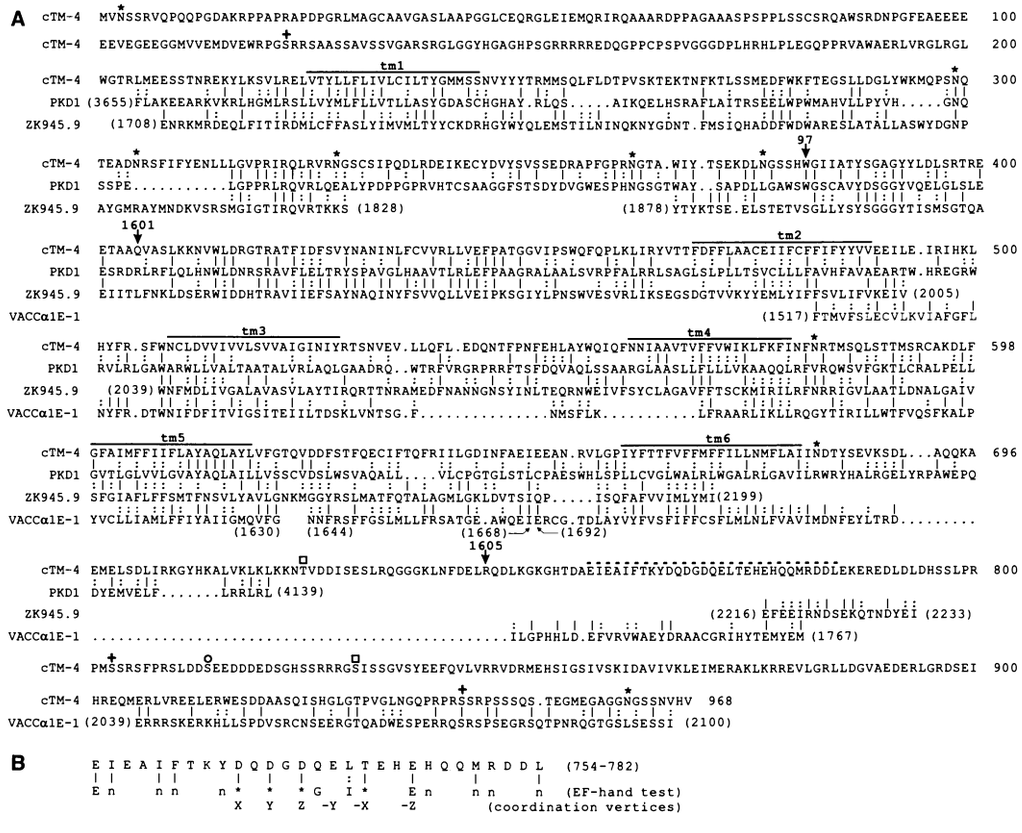

Fig. 4. Deduced amino acid sequence of PKD2 (*19*). (**A**) Alignment of cTM-4 with PKD1 (gb|U24497), the *C. elegans* homolog of PKD1 (ZK945.9; swiss| Q09624), and VACCα_{1E-1} (pir|B54972) from BESTFIT (*32*): identity to cTM-4 is indicated with a vertical line and similarity to cTM-4 with two dots (:). Numbers in parentheses refer to amino acids in respective sequences. The putative transmembrane domains are tm1 to tm6 (*22*). Predicted *N*-glycosylation sites are marked with an asterisk. Potential phosphorylation sites with strong consensus sequences are marked as follows: plus sign, phosphorylation by protein kinase C; open square, phosphorylation by guanosine 3′,5′-cyclic monophosphate–dependent kinase (Ser^{826} is also consistent with a protein kinase A site); and open circle, phosphorylation by casein kinase. The sites of the nonsense mutations (Fig. 3) are indicated by arrows labeled with the respective family numbers. The EF-hand domain is in-icated by the dashed line. (**B**) Alignment of the EF-hand domain with the EF-hand test sequence (*24*). The residues E, G, I, and E, the latter being a Ca^{2+} coordination vertex, are the expected residues at the indicated positions in the EF-hand. Positions indicated as "n" are expected to have hydrophobic amino acids (L, I, V, F, M); those denoted with an asterisk should be oxygen-containing amino acids (D, N, E, Q, S, T) making up the remainder of coordination vertices for Ca^{2+} binding; the -Y vertex can be any amino acid. The Leu (L) in PKD2 in place of the Ile (I) is likely a permissible substitution (*24*); PKD2 has Gln (Q) in place of the consensus Gly (G) as is the case with EF-hand domains in the α_1 Na^+ channels (*24*). Abbreviations for the amino acid residues are as follows: A, Ala; C, Cys; D, Asp; E, Glu; F, Phe; G, Gly; H, His; I, Ile; K, Lys; L, Leu; M, Met; N, Asn; P, Pro; Q, Gln; R, Arg; S, Ser; T, Thr; V, Val; W, Trp; and Y, Tyr.

IV), each with six transmembrane spans (S1 to S6), which are predicted to form the pore structure (*25, 26*). The membrane spans tm2 through tm6 as well as the intervening intracellular loops of PKD2 have similarity with corresponding segments in the α_1 channels (Fig. 4) (*25*). The similarity in the COOH-terminal region includes the putative EF-hand domain (Fig. 4) (*24*). This domain in PKD2 scores highly on the EF-hand test (Fig. 4B), with identity at all the critical coordination vertices (*24*). EF-hand domains are specialized helix-loop-helix motifs that have Ca^{2+} binding activity in ~70% of the proteins in which they occur (*27*). Unpaired EF-hand sequences have recently been implicated in Ca^{2+}-sensitive inactivation of some forms of L-type VACCα_1 (*28*). EF-hand domains that do not coordinate Ca^{2+} remain important to protein function (*24, 29*).

Despite the observed homology to PKD1, the predicted structure of the PKD2 protein does not directly suggest a role in cell-cell or matrix-cell signaling similar to that proposed for PKD1 (*17, 18*). PKD2 does not have the large NH_2-terminal extracellular domain and the associated motifs found in PKD1 (*17, 18*). It is possible that PKD2 functions in a parallel pathway with PKD1. However, given that the clinical diseases produced by mutations in *PKD1* and *PKD2* exhibit an identical spectrum of organ involvement, differing only in relative rates of progression of cystic changes, hypertension, and the development of end-stage renal disease, the most likely scenario is that PKD2 associates with itself, with PKD1, or with other proteins and ligands as part of a common signal transduction pathway.

PKD2 bears some similarity to the α_1 Ca^{2+} (and Na^+) channels but has only six membrane spans. If it formed homo- or heteromultimeric complexes (for example, with itself, with the homologous portion of PKD1, or with another protein), it could function as an ion channel or pore in a manner similar to the K^+ channels (*26*). The observed homologies, the presence of a pair of conserved basic residues (Lys^{573} and Lys^{576}) in the fourth transmembrane domain, and the predicted even number of membrane spans are consistent with such a role (*26*). In such a model, PKD1 could act as the regulator of the PKD2 channel activity, perhaps with Ca^{2+} as a second messenger in a signal transduction pathway. The discovery of PKD2 raises the possibility that the ADPKD phenotype may in part be the result of a defect in an unknown transport function.

REFERENCES AND NOTES

1. P. A. Gabow, *N. Eng. J. Med.* **329**, 332 (1993).
2. _____ *et al.*, *Kidney Int.* **38**, 1177 (1990); A. B. Chapman *et al.*, *N. Eng. J. Med.* **327**, 916 (1992); K. F. Hossack, C. L. Leddy, A. M. Johnson, R. W. Schrier, P. A. Gabow, *ibid.* **319**, 907 (1988); V. E. Torres, D. M. Wilson, R. R. Hattery, J. W. Segura, *Am. J. Kidney Dis.* **22**, 513 (1993); J. Huston, V. E. Torres, P. P. Sulivan, K. P. Offord, D. O. Wiebers, *J. Am. Soc. Nephrol.* **3**, 1871 (1993); S. Somlo *et al.*, *ibid.* **4**, 1371 (1993).
3. W. J. Kimberling *et al.*, *N. Eng. J. Med.* **319**, 913 (1988).
4. S. T. Reeders *et al.*, *Nature* **317**, 542 (1985); G. Romeo *et al.*, *Lancet* ii, 8 (1988); M. C. Daoust, D. M. Reynolds, D. G. Bichet, S. Somlo, *Genomics* **25**, 733 (1995); S. de Almeida *et al.*, *Hum. Genet.* **96**, 83 (1995).
5. W. J. Kimberling *et al.*, *Genomics* **18**, 467 (1993); D. J. M. Peters *et al.*, *Nature Genet.* **5**, 359 (1993).
6. D. J. M. Peters and L. A. Sandkuijl, *Contrib. Nephrol.* **97**, 128 (1992).
7. P. S. Parfrey *et al.*, *N. Eng. J. Med.* **323**, 1085 (1990); D. Ravine *et al.*, *Lancet* **340**, 1330 (1992).
8. F. S. Collins, *Nature Genet.* **1**, 3 (1992); *ibid.* **9**, 347 (1995).
9. OMIM (On-line Mendelian Inheritance in Man) number 173910.
10. T. Mochizuki *et al.*, unpublished observations; B. Veldhuisen *et al.*, unpublished observations.
11. T. Mochizuki *et al.*, *J. Am. Soc. Nephrol.* **5**, 631a (1994); J. L. San Millan *et al.*, *Am. J. Hum. Genet.* **56**, 248 (1995); D. J. M. Peters *et al.*, *ibid.* **57**, 200a (1995).
12. C. D. Constantinou-Deltas *et al.*, *Hum. Genet.* **95**, 416 (1995).
13. O. Riess *et al.*, *Cytogenet. Cell Genet.* **65**, 238 (1994); P. A. Ioannou *et al.*, *Nature Genet.* **6**, 84 (1994).
14. Cosmid and P1 contig construction in this region was guided by the existing YAC contig (*10*). Cosmid clones were obtained by hybridization screening of the human chromosome 4–specific cosmid library (*13*). The probes used for hybridization were (i) pooled *Alu* products from mega-YAC 967d1, (ii) end sequences from cosmid or P1 clones mapping into the region, and (iii) internal restriction fragments from the YAC, P1, and cosmid clones. All hybridization probes were labeled with [α-^{32}P]deoxycytidine 5′-triphosphate (dCTP) by standard techniques. Human repetitive sequences were precompeted with 30 to 80 μg of COT-1 DNA (Gibco-BRL, Gaithersburg, MD) using the manufacturer's protocol. Hybridization was carried out in Church-Gilbert buffer. The P1 library (*13*) was screened by PCR from colony pools of each 384-well plate with STS4-1078 (*SPP1*) and D4S1171. Cosmid and P1 clones mapping into the *PKD2* interval were screened for STS content to anchor positive clones onto the YAC contig. Overlap relations among the clones were established by Eco RI fingerprint analysis and by hybridization.
15. A total of 6×10^5 plaques of oligo(dT) and random-primed human fetal brain (Stratagene number 936206) and adult kidney (Clonetech number HL3001a) cDNA libraries were plated at a density of 3×10^4 per 150-mm plate and replica lifted onto nylon filter circles. Cosmid and P1 inserts used in library screening were released from the vector with Not I and purified from agarose gels. The cumulative length of the inserts used as a probe in a library screening was <80 kb to maintain an adequate signal-to-noise ratio. Insert DNA was labeled and precompeted with 2 μg of sCOS-1 vector in addition to COT-1 DNA. Positively hybridizing plaques were purified by standard techniques, and insert DNA was excised (λZAPII) or subcloned (λgt10).
16. S. F. Altschul, W. Gish, W. Miller, E. W. Myers, D. J. Lipman, *J. Mol. Biol.* **215**, 403 (1990).
17. The European Polycystic Kidney Disease Consortium, *Cell* **77**, 881 (1994); The International Polycystic Kidney Disease Consortium, *ibid.* **81**, 289 (1995); The American PKD1 Consortium, *Hum. Mol. Genet.* **4**, 575 (1995).
18. J. Hughes *et al.*, *Nature Genet.* **10**, 151 (1995).
19. GenBank accession number gb|U50928.
20. M. Kozak, *Nucleic Acids Res.* **15**, 8125 (1987).
21. The mutation in family 1605 was detected initially in a reverse transcriptase–PCR (RT-PCR) template by using the cDNA-based primers F11 (5′-GGGCTACCATAAAGCTTTG-3′) and R11 (5′-GTTCATGTTCGATCAGTTCT-3′) (205-bp product) and confirmed in genomic DNA by using F11 with intronic primer IR11 (5′-GGGCTAGAAATACTCTTATCACC-3′) (201-bp product). The mutations in families 97 and 1601 were initially detected in genomic DNA with intronic primers IF1C (5′-GCCTCAAGTGTTCCACTGAT-3′) and IR1 (5′-AGGTTTTTCTGGGTAACCCTAG-3′) (362-bp product). Amplifications were performed in standard conditions with Hot Start. Products were labeled by [α-^{32}P]dCTP incorporation, diluted, and denatured in formamide buffer before electrophoresis. SSCA was performed according to published protocols [M. Orita, Y. Suzuki, T. Sekiya, K. Hayashi, *Genomics* **5**, 874 (1989)]. Sequencing of purified PCR products was performed with either an ABI 373a or ABI 377 automated sequencing apparatus with cycle sequencing with dye terminator chemistries according to the manufacturer's protocol. The PCR primers were used as sequencing primers, and all products were sequenced in both directions. The mutation in family 97 results in the loss of a Bsr I site. Genomic DNA amplified with IF1C and IR1 and digested with Bsr I yields products of 261 and 101 bp in the normal allele. The mutation in family 1605 results in the loss of a Taq I site. Genomic DNA amplified with F11 and IR11 and digested with Taq I yields products of 105 and 96 bp in the normal allele. The SSCA conditions used to demonstrate the mutation in the IF1C-IR1 genomic PCR product in family 1601 were 6% acrylamide (29:1, acrylamide: *bis*-acrylamide) and 1×tris-borate EDTA (TBE), on a 20-cm gel run at 14°C and 100 V for 6 hours.
22. B. Rost, R. Casadio, P. Fariselli, C. Sander, *Protein Sci.* **4**, 521 (1995); P. Klein, M. Kanehisa, C. DeLisi, *Biochim. Biophys. Acta* **815**, 468 (1985); J. Kyte and R. F. Doolittle, *J. Mol. Biol.* **157**, 105 (1982); D. M. Engelman, T. A. Steitz, A. Goldman, *Annu. Rev. Biophys. Biophys. Chem.* **15**, 321 (1986).
23. L. Sipos and G. von Heijne, *Eur. J. Biochem.* **213**, 1333 (1993); H. Nakashima and K. Nishikawa, *FEBS Lett.* **303**, 141 (1992); E. Hartmann, T. A. Rapoport, H. F. Lodish, *Proc. Natl. Acad. Sci. U.S.A.* **86**, 5786 (1989).
24. R. H. Kretsinger, *Cold Spring Harb. Symp. Quant. Biol.* **52**, 499 (1987); J. Babitch, *Nature* **346**, 321 (1990).
25. M. E. Williams *et al.*, *J. Biol. Chem.* **269**, 22347 (1994); M. E. Williams *et al.*, *Science* **257**, 389 (1992); T. W. Soong *et al.*, *ibid.* **260**, 1133 (1993); W. A. Horne *et al.*, *Proc. Natl. Acad. Sci. U.S.A.* **90**, 3787 (1993).
26. B. Hille, *Ionic Channels of Excitable Membranes* (Sinauer Associates, Sunderland, MA, ed. 2, 1992), pp. 250–257.
27. S. Nakayama and R. H. Kretsinger, *Annu. Rev. Biophys. Biomol. Struct.* **23**, 473 (1994).
28. M. de Leon *et al.*, *Science* **270**, 1502 (1995).
29. J. Gulati, A. Babu, H. Su, *J. Biol. Chem.* **267**, 25073 (1992).
30. D. Cohen, I. Chumakov, J. Weissenbach, *Nature* **366**, 698 (1993).
31. M. B. Soares *et al.*, *Proc. Natl. Acad. Sci. U.S.A.* **91**, 9228 (1994).
32. BESTFIT, Program Manual for the Wisconsin Package, version 8, September 1994.

33. We thank R. Kucherlapati, V. Schuster, G. Germino, B. Morrow, and the Kucherlapati laboratory for helpful discussions; G.-J. van Ommen for support; L. Deaven for the chromosome 4–specific cosmid library; D. Lepaslier for YAC clones; J. L. San Millan, S. Gerken, J. Murray, M. Dixon, and J. Weissenbach for STSs; and G. Grills for help with sequencing. Supported by grants from NIH (DK48383, DK02015), the American Heart Association (94015510), the March of Dimes Birth Defects Foundation, the Marion Merrell Dow Award from the Polycystic Kidney Research Foundation, the American Federation for Clinical Research, the Albert Einstein Human Genome Program (S.S.), a Martin Foundation Fellowship (T.M.), the Cyprus Kidney Foundation (C.C.D.), and the Dutch Kidney Foundation (B.V. and J.S.).

1 February 1996; accepted 21 March 1996